



## Chemical Composition of Fog Water at Four Sites in Taiwan

Stefan Simon<sup>1\*</sup>, Otto Klemm<sup>1</sup>, Tarek El-Madany<sup>1</sup>, Joschka Walk<sup>1</sup>, Katharina Amelung<sup>1</sup>,  
Po-Hsiung Lin<sup>2</sup>, Shih-Chieh Chang<sup>3</sup>, Neng-Huei Lin<sup>4</sup>, Guenter Engling<sup>5,6</sup>, Shih-Chieh Hsu<sup>7</sup>,  
Tsong-Huei Wey<sup>8</sup>, Ya-Nan Wang<sup>9</sup>, Yu-Chi Lee<sup>10</sup>

<sup>1</sup> *Climatology Working Group, Institute of Landscape Ecology, University of Münster, Germany*

<sup>2</sup> *Department of Atmospheric Sciences, National Taiwan University, Taipei, Taiwan*

<sup>3</sup> *Department of Natural Resources and Environmental Studies, National Dong Hwa University, Hualien, Taiwan*

<sup>4</sup> *Department of Atmospheric Sciences, National Central University, Chung-Li, Taiwan*

<sup>5</sup> *Department of Biomedical Engineering and Environmental Sciences, National Tsing Hua University, Hsinchu, Taiwan*

<sup>6</sup> *Division of Atmospheric Sciences, Desert Research Institute, Reno, NV, USA*

<sup>7</sup> *Trace Element Laboratory, Research Center for Environmental Changes, Academia Sinica, Taipei, Taiwan*

<sup>8</sup> *The Experimental Forest, National Taiwan University, Jhu-Shan, Nantou, Taiwan*

<sup>9</sup> *School of Forest and Resource Conservation, National Taiwan University, Taipei, Taiwan*

<sup>10</sup> *Central Weather Bureau, Taipei, Taiwan*

---

### ABSTRACT

This study characterizes and compares the chemical composition of fog water at four sites in Taiwan. Fog was sampled with identical active fog collectors (modified Caltech design) using identical sampling strategies at all four sites. While the sites varied largely in terms of altitude above mean sea level (asl), type of fog, and the potential sources of constituents in fog water, the chemical composition of fog water was in all cases clearly dominated by  $\text{H}^+$ ,  $\text{NH}_4^+$ ,  $\text{NO}_3^-$  and  $\text{SO}_4^{2-}$ , making up more than 85% of the total ion concentrations. The pH ranged from 2.27 to 5.95.

Sulfur dioxide emissions from coal combustion in Mainland China and Taiwan as well as nitrogen oxide emissions from urbanized central-west Taiwan and the greater Taipei region were the main precursors of fog acidity. Ammonia, originating from agriculture emissions, was the main neutralizer. The Kinmen site (48 m asl), situated on an island close to Mainland China, exhibited the lowest pH and the highest sulfate concentrations. At the Xitou site on the western slopes of the Taiwan Central Mountain Range (1150 m asl), ammonium from agriculture dominated and lead to relatively high pH. At the same time, the nitrate/sulfate ratio was highest at this site ( $> 1$  in equivalent units), resulting from relatively large contributions from street traffic. The ion concentrations at the Chilán site (1650 m asl) and the Lulin high mountain site (2862 m asl) were much lower than those at Xitou and Kinmen. While the ion concentrations at Chilán were considerably lower than at Lulin, the ion loadings, which is the amount of dissolved ions per volume of air, were similar at Chilán and Lulin.

**Keywords:** Cloud; Fog chemistry; Fog collection; Taiwan; Air pollution.

---

### INTRODUCTION

Fog is a lower-atmospheric near-surface cloud, consisting of liquid or solid hydrometeor particles suspended in air (Yang *et al.*, 2011). It is a very complex and dynamic medium allowing both the reorganization and the removal of particle mass (Li *et al.*, 2011), whereby the sources, formation processes, transport corridors of these particles in moist air (Seinfeld and Pandis, 2006), their dissolution in liquid water as well as their aqueous reactivity, and eventually the

evaporation of fog droplets and their deposition to the surface determine the fog's chemistry. In addition, the deposition of fog droplets to the underlying surface has an impact on the average chemical composition of the liquid water as does the evaporation during the dissipation phase of a fog event (Degefie *et al.*, 2015).

The field of fog research is comparatively young, while first studies on fog water chemistry started in the beginning of the 1900s (Herckes *et al.*, 2015) and have received more and more attention since the 1980s (Yang *et al.*, 2011). The collection of fog is quite challenging and time consuming. Nevertheless, numerous studies investigated the chemical composition of fog in the United States (e.g., Collett *et al.*, 1999a, b; Collett *et al.*, 2002; Herckes *et al.*, 2015), in Europe (e.g., Wrzesinsky and Klemm, 2000; Polkowska *et al.*, 2008;

---

\* Corresponding author.

Tel.: +49 (0) 251 83 33912; Fax: +49 (0) 251 83 38338  
E-mail address: stefansimon@uni-muenster.de

Giulianelli *et al.*, 2014; Wang *et al.*, 2015), and in Asia (e.g., Tago *et al.*, 2006; Kim *et al.*, 2006; Watanabe *et al.*, 2006; Lu *et al.*, 2010; Watanabe *et al.*, 2010; Li *et al.*, 2011; Yang *et al.*, 2011).

There is a close relation between chemical characteristics of fog water and atmospheric pollutants (Yang *et al.*, 2011), suggesting that fog water may be heavily impacted in some areas of East Asia, where emissions are high due to the intense combustion of fossil fuels, high density of industrial emission sources, and low emission control standards.

To study the contamination of fog water by pollutants as emitted in East Asia, Taiwan is the ideal investigation area. The subtropical island features very humid air and a high Central Mountain Range almost over its entire north-south extension. Many of its mid- and highland cloud forests experience more than 100 days of fog per year, while there are more than 250 days of fog per year reported for mountains higher than 2000 m above mean sea level (asl) such as Mt. Ali, Mt. Lulin, and Mt. Yu (Liang *et al.*, 2009). Studies of fog chemistry in Taiwan did not start until the 1990s, while only limited data is published from Mount Bamboo (Lin and Peng, 1998; Lin *et al.*, 2010), Chilan Mountain (Chang *et al.*, 2002; Beiderwieden *et al.*, 2007), and Xitou Experimental Forest (Liang *et al.*, 2009).

Lin and Peng (1998) collected fog water on an hourly basis during 1996 and 1997 at Mt. Bamboo and reported pH values between 2.63 and 6.43. They continued their investigations and Lin *et al.* (2010) presented pH values between 3.21 and 5.85, with a mean of 4.26 based on 4589 samples from 130 events. During the 15-year-period between 1996 and 2010, the dominant ions were  $\text{Na}^+$ ,  $\text{Cl}^-$ ,  $\text{SO}_4^{2-}$ ,  $\text{NO}_3^-$  and  $\text{NH}_4^+$ , while most of the air masses were advected from Mainland China. For the Yuan-Yang Lake area in northeastern Taiwan, Chang *et al.* (2002) reported annual median and minimum pH values of fog water of 4.3 and 3.3. At the same site, nowadays known as Chilan Mountain Site (CLM), Beiderwieden *et al.* (2007) presented median and minimum pH values of 4.13 and 2.24, while  $\text{H}^+$ ,  $\text{NH}_4^+$ ,  $\text{NO}_3^-$  and  $\text{SO}_4^{2-}$  contributed 85% to the total equivalent ion concentration. For Xitou (XT), Liang *et al.* (2009) reported an annual median pH of 4.9 of fog water with  $\text{SO}_4^{2-}$  and  $\text{NH}_4^+$  being the dominating ions. Overall, the data available for Taiwan is still relatively sparse. Further, it needs to be recognized that the employed sampling techniques and procedures have a strong influence on the measured fog chemistry. For example, the operational status of the collector (on/off) during non-foggy conditions, the visibility at which the collector is switched, the fog collector cleaning procedure before the onset of a fog event, and the sample integration periods have an influence on the measured fog water chemistry and often impair the comparability of results between studies. So far no investigators have attempted to employ similar sampling designs at several locations of Taiwan in order to compare them among each other.

This paper presents the investigation of fog samples as taken at four sites in Taiwan (i) to assess first-time data on the chemical composition of fog water at Lulin Mountain and Kinmen Island, (ii) to carefully determine the chemical characteristics of fog at Chilan Mountain, Lulin Mountain,

Xitou Experimental Forest and Kinmen Island as sampled with an identical setup and sample design, (iii) to identify the source regions of air pollution contributing to high pollutant concentrations in fog water, and (iv) to study the role of dilution within the fog liquid phase on the measurable ion concentrations

## EXPERIMENTAL

### Site Description

Fog collectors were set up at four different sites in Taiwan, including the Chilan Mountain Research Station (CLM; 24°35'27"N, 121°29'56"E, 1650 m asl), the Lulin Atmospheric Background Station (LABS; 23°28'06"N, 120°52'25"E; 2862 m asl), the Xitou Flux Tower in the Experimental Forest of National Taiwan University (XT; 23°39'52"N, 120°47'43"E, 1150 m asl) and the Kinmen Weather Station (KM; 24°24'26"N, 118°17'21"E, 48 m asl) (see Fig. 1).

While all samples were taken with the same type of fog collector, instrument setup and experimental design, the sites vary largely with respect to altitude above sea level, type of fog and the potential sources of constituents in fog water.

At CLM, samples were taken between April 13<sup>th</sup> 2011 and May 24<sup>th</sup> 2011. The physics and chemistry of fog has been studied by Chang *et al.* (2006), Beiderwieden *et al.* (2007), Gonser *et al.* (2011), and El-Madany *et al.* (2013) at a meteorological tower extending about 10 m above the canopy height. The tower is surrounded by a 300 ha homogenous yellow cypress plantation with an average height of 14.8 m (Beiderwieden *et al.*, 2007), a largely homogenous canopy, and a slope of 14% (Chang *et al.*, 2006). As at all sites, the general climate at CLM is characterized by two subtropical East Asian Monsoons. The so-called summer monsoon is associated with a southwesterly flow and typically lasts from May until early September, while the northeast winter monsoon lasts from September until about March. Further, typhoons quite frequently hit Taiwan between the months of August and October (Lai *et al.*, 2006; Hsu *et al.*, 2010), leading to an average annual precipitation of more than 3000 mm. The average annual air temperature is 12.7°C (Lai *et al.*, 2006). The site is characterized by a well-pronounced regular daily wind regime with a valley wind from SE during daytime and a mountain wind from N to NW during the nights. The valley wind occurs usually in combination with fog (Chang *et al.*, 2006). For this study, the fog collector was setup at a height of 21 m above ground and oriented towards SE, directly pointing into the bottom of the valley.

At LABS, samples were taken between April 13<sup>th</sup> 2011 and May 17<sup>th</sup> 2011. The LABS site lies frequently in the free troposphere, especially during the winter season, and is therefore generally free from boundary layer pollution (Wai *et al.*, 2008). Within a 50 km-radius of the sampling site, there are only small villages spread over the mountain range. The nearest major city, Taichung, lies approximately 90 km to the Northwest. The annual mean temperature is 10°C, with highest monthly mean temperature in July (14°C) and lowest in January (5°C). The average annual

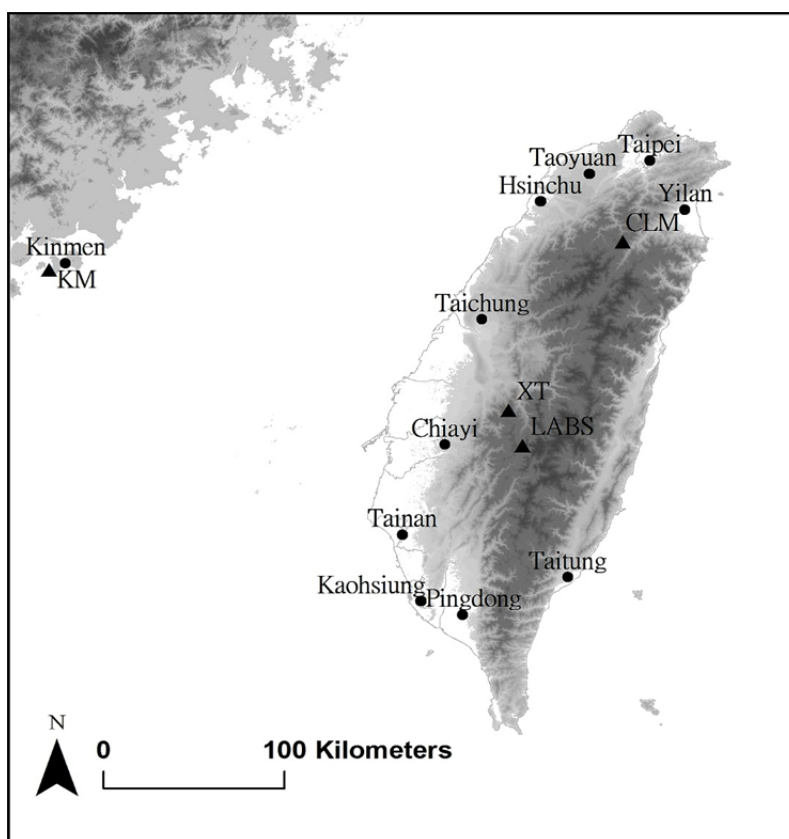


**Fig. 1.** Map of Taiwan, including the four experimental sites Chilan Mountain Research Station (CLM), Lulin Atmospheric Background Station (LABS), the Xitou Flux Tower in the Experimental Forest of National Taiwan University (XT), and the Kinmen Weather Station (KM). The plains to the West of the Central Mountain Range are heavily populated with extensive industrial and agricultural activity, while the Eastern coastline is relatively sparsely developed. (Map created with ArcGIS® software by Esri using ASTER GDEM data)

precipitation exceeds 4000 mm per year (Sheu *et al.*, 2010). The measurement was performed on the rooftop of the two-story LABS building at 6 m above ground level. The fog collector was manually oriented into the main wind direction during fog occurrence.

At XT, samples were taken between September 9<sup>th</sup> 2013 and November 1<sup>st</sup> 2013. The meteorological tower is situated in a coniferous forest, dominated by *Cryptomeria japonica*. The mean annual temperature is 16.6°C, with a mean maximum of 20.8°C in July and a mean minimum of 12.0°C in January. The mean annual precipitation of 2635 mm is divided into two seasons, a dry season from October to April, and a wet season from May to September. The XT site is located in a relatively flat section (slope of 15°) of a valley with orientation from N to S.

The site is not more than 15 km away from the heavily industrialized urban area of central-western Taiwan. Besides tourism, the high-lying region of Xitou is intensively used for agriculture, along with heavy fertilizer input (Liang *et al.*, 2009). The site is characterized by a quite regular daily wind regime. A valley wind from N occurs predominantly during daytime and a mountain wind from S during nights. Dense orographic fog occurred mainly during daytime as driven by the valley wind. The fog collector was set-up at a height of about 37 m above ground and oriented towards

N, pointing into the valley.

At KM, samples were taken between March 27<sup>th</sup> 2014 and April 13<sup>th</sup> 2014. The Kinmen Weather Station is located in the southwest corner of Kinmen Island, Taiwan. The Island is located close to Fujian Province, China, and therefore rather directly exposed to pollution transport from Mainland China (Lee *et al.*, 2011). The region is marked by a marine climate (Hsu *et al.*, 2010), with an annual mean temperature of 20.9°C, with the maximum in August and the minimum in January. The average annual precipitation is 1072 mm and is concentrated between April and September. The fog collector was set up at a height of about 6 m above ground and manually oriented into the wind. During the experimental period, the fog type was an ocean steam fog which was driven by winds from S and SSW towards the station.

#### **Fog Collection**

At all investigated sites the same type of fog collector and instrument setup was used. An active fog collector, consisting of a fan unit and a fog collection unit, was modified after Klemm *et al.* (2008). The fog collection unit is completely made up of inert materials, PEEK (*polyether ether ketone*) and PTFE (*polytetrafluoroethylene*), to prevent contamination from construction material and sampling lines in terms of ions and metals. More details on the fog

collector are given in Degeffie *et al.* (2015).

The fog collector was complemented by a present weather detector (model PWD11, Vaisala OY, Finland) to measure visibility. When the visibility reached a value below 1000 m, the fog collector automatically started collecting fog water. Samples were removed manually as soon as there was sufficient collected fog water for all chemical analyses. Fog water was collected in a covered 2 L high density polyethylene (HDPE) bottle. After completion of a sample, the water was distributed over two 15 mL HDPE bottles, of which one was acidified with HNO<sub>3</sub> to keep metals in solution for their analysis. Shortly after the samples were taken, the bottles were stored in a freezer and later shipped to the lab. To ensure quality of the data and to eliminate contamination of the samples during field work, transport, storage and analytical procedures, two types of blank samples were taken. Fog collector blanks ensure the adequacy of collector cleaning by spraying deionized-water into the sampling unit while the fan is running. Deionized-water blanks control the quality of the used deionized-water, while aliquots are directly filled into sampling bottles without getting in contact with the fog collector. Afterwards blanks were treated like normal samples.

### Chemical Analysis

Directly after collection of individual fog water samples, their volume was determined gravimetrically and pH and conductivity were measured electrometrically. The samples were later analyzed for Na<sup>+</sup>, NH<sub>4</sub><sup>+</sup>, K<sup>+</sup>, Mg<sup>2+</sup>, Ca<sup>2+</sup>, Cl<sup>-</sup>, NO<sub>3</sub><sup>-</sup>, PO<sub>4</sub><sup>3-</sup>, SO<sub>4</sub><sup>2-</sup>, as well as Al, Fe, Ti, V and Se. Organic ions were not measured. Chemical analysis of fog water was conducted at the Institute of Landscape Ecology at the University of Münster in Germany (Beiderwieden *et al.*, 2007) for CLM and LABS, at the Department of Biomedical Engineering and Environmental Sciences at National Tsing Hua University in Taiwan (Zhang *et al.*, 2015) for XT, and at the Research Center for Environmental Changes, Academia Sinica, Taipei in Taiwan (Hsu *et al.*, 2010) for KM. All samples were filtered directly before analysis. Ion Chromatography (IC) was used for ion analysis and Inductively Coupled Plasma Mass Spectrometry (ICP-MS) for the analysis of Al, Fe, Ti, V and Se.

Most ion concentrations in fog were well above the analytical detection limits. Blank samples confirmed that there was no contamination of fog water. Fog samples that did not meet the ion balance criteria of the World Meteorological Organization (WMO) for precipitation water (WMO 2004), were excluded from further analysis. Only in very few cases, when individual samples were within a temporal sequence within a single fog event and the samples were apparently consistent with the preceding and following samples, somewhat larger dis-closures of the ion balance were accepted. This is justifiable before the background that accepted ion balances almost exclusively were positive, while the non-closure of the calculated ion balance may be caused by ions in the sample that were not analyzed such as carboxylic acid anions in our case. Further, the comparison of the measured conductivity with the conductivity as calculated from the total of individual ion conductivities

were used as quality criteria (WMO 2004).

It has long been reported that H<sub>2</sub>SO<sub>4</sub> and HNO<sub>3</sub> are the major acids in fog water (e.g., Jacob *et al.*, 1986, Johnson *et al.*, 1987; Joos and Baltensperger, 1991, Tago *et al.*, 2006). Hara (1993) and Hara *et al.* (1995) proposed the parameter pAi to express the un-neutralized acidity of fog water, which is semi-quantitatively defined as the equivalent concentrations of non-sea-salt-sulfate (nss-SO<sub>4</sub><sup>2-</sup>) plus nitrate ions (Polkowska *et al.*, 2008):

$$pAi = -\log\left(\left[nss - SO_4^{2-}\right] + \left[NO_3^-\right]\right) \quad (1)$$

Square brackets indicate equivalent concentrations. Hara *et al.* (1995) describe pAi as “the minimum pH under the condition that no neutralizing agents such as ammonia and alkaline calcium salts were incorporated into the water droplet in its history before hitting the earth’s surface”.

To represent the ratio of un-neutralized H<sup>+</sup> in liquid water, Daum *et al.* (1984) proposed the fractional acidity (FA) as an indicator:

$$FA = \frac{\left[H^+\right]}{\left[nss - SO_4^{2-}\right] + \left[NO_3^-\right]} \quad (2)$$

By assuming that all the hydrogen ions in fog water originate from acidic input of H<sub>2</sub>SO<sub>4</sub> and HNO<sub>3</sub>, and no neutralization of these acids happened, FA would be unity (Lu *et al.*, 2010).

To identify the individual impact of a cation X on the neutralization of acidity, Ali *et al.* (2004) defined the neutralization factor (NF) of X as:

$$NF(X) = \frac{\left[nss - X^+\right]}{\left[nss - SO_4^{2-}\right] + \left[NO_3^-\right]} \quad (3)$$

where “X” is the neutralizing cation and [nss-X<sup>+</sup>] is its non-sea-salt equivalent concentration.

An inverse relationship between measured ion concentrations and liquid water content (LWC) of clouds was observed by Elbert *et al.* (2000). In our study, the LWC in mg m<sup>-3</sup> was calculated for each sample by the fog water collection rate (FCWR) in mg min<sup>-1</sup> divided by the product of the fog collectors fog collection efficiency (FCE) and flow rate (FR):

$$LWC = \frac{FCWR}{FCE \times FR} \quad (4)$$

where the fog collection efficiency is 88% and the flow rate is 17.65 m<sup>3</sup> min<sup>-1</sup>.

To consider the dilution of ions by water, the liquid phase concentrations of ions (ICs) were transformed into atmospheric ion loadings (ILs). The ion loading is defined as the amount of ions dissolved in the liquid phase within 1 m<sup>3</sup> air. It is calculated as

$$IL(i) = \frac{LWC \times [IC(i)]}{\rho} \quad (5)$$

where  $\rho$  is the density of water ( $1000 \text{ kg m}^{-3}$ ),  $[IC(i)]$  is the ionic concentration of all measured species  $i$  in fog water (see Table 1) in units  $\mu\text{eq L}^{-1}$ , LWC is the liquid water content in units  $\text{g m}^{-3}$ , and  $IL(i)$  is given in units  $\mu\text{eq m}^{-3}$ , respectively.

### Air Mass Backward Trajectories

Trajectories describe the tracks along which air masses move within the atmosphere. The analysis of air mass backward trajectories is widely used to study the advection and potential source regions of air pollutants. We analyzed 48-hour backward trajectories using the Hybrid Single-Particle Lagrangian Integrated Trajectory model (Draxler and Hess, 1998), as provided by the Air Resources Laboratory of NOAA at <http://www.arl.noaa.gov/HYSPLIT.php>. For the computation the Global Data Assimilation System (GDAS) of the National Centers for Environmental Prediction (NCEP) was chosen. Every fog event is represented by one to five trajectories depending on its duration (Fig. 3).

## RESULTS AND DISCUSSION

### Ion and Metal Concentrations in Fog Water

Table 1 lists the statistics of fog water samples, the ion concentrations and derived indicators, as well as the metal concentrations that were analyzed for all sites. For the sites CLM, LABS, and XT, the numbers of fog events and the numbers of samples are rather similar to each other. At KM, only two fog events occurred during the experimental campaign, however, a total number of 15 samples was collected. Although samples were taken in different years and seasons, we consider the sample populations to be comparable to each other.

The dominant ions in the fog water at all four sites were  $\text{H}^+$ ,  $\text{NH}_4^+$ ,  $\text{NO}_3^-$  and  $\text{SO}_4^{2-}$ , with their medians making up more than 85% of the median total ion concentrations (TIC) of the fog water at each site (CLM: 86%, LABS: 95%, XT: 86%, KM: 92%). Similar conditions are reported for other sites in Taiwan (Beiderwieden *et al.*, 2007; Liang *et al.*, 2009; Lin *et al.*, 2010) as well as many sites all over the world (e.g., Wrzesinsky and Klemm, 2000; Collett *et al.*, 2002; Tago *et al.*, 2006; Li *et al.*, 2011; Giulianelli *et al.*, 2014; Herckes *et al.*, 2015; Wang *et al.*, 2015).

The ammonium concentrations in fog water mainly represent the input from the precursor gas ammonia (Collett *et al.*, 2002), which is emitted from near-surface sources, particularly by local anthropogenic emissions such as agricultural activities, human waste, and traffic emissions (Li *et al.*, 2011). In terms of percentage, the median  $\text{NH}_4^+$  concentrations contribute 40% at CLM, 39% at XT, 30% at LABS, and 15% at KM to the total ion concentration. At CLM, XT, and LABS,  $\text{NH}_4^+$  was the cation with the highest concentrations; only at KM the  $\text{H}^+$  concentration was higher.

Nitrate derives from the scavenging of aerosol nitrate and the uptake of gaseous nitric acid (Collett *et al.*, 2002). The sources of these  $\text{NO}_3^-$  precursors are mainly nitrogen

oxide (NO) emissions from vehicular exhaust and fossil-fuel power stations (Lu *et al.*, 2010). In terms of percentage, median  $\text{NO}_3^-$  concentrations ranged from 13% at KM to 21% at XT.

Sulfate is the predominant acidifying pollutant of fog water at many sites in Asia (Kim *et al.*, 2006; Li *et al.*, 2011; Yang *et al.*, 2011). It is formed by atmospheric oxidation from its precursor sulfur dioxide ( $\text{SO}_2$ ). The atmospheric  $\text{SO}_2$  mainly originates from the burning of sulfur-rich fossil fuels. Some sulfate also originates from sea salt, which may, under certain conditions, exert an important contribution to the ion composition in fog. The non-sea-salt-sulfate ( $\text{nss-SO}_4^{2-}$ ) concentration was calculated from the sulfate concentration in fog, the sodium concentration, and the average ratio of these ions in sea water (see Table 1 for more details). The  $\text{nss-SO}_4^{2-}$  to total sulfate ratios were very high, above 99%, at all sites, showing that it is anthropogenic sulfur emissions that dominate the  $\text{SO}_4^{2-}$  concentration in fog. The median fraction of  $\text{SO}_4^{2-}$  to total anion concentrations ranged between 45% at XT and 62% at KM, while the absolute value of the median  $\text{SO}_4^{2-}$  concentrations in KM was nearly four times higher than that at LABS, and nearly fifteen times higher than that at CLM.

The  $\text{NO}_3^-/\text{SO}_4^{2-}$  - ratio is a widely used parameter (Collett *et al.*, 2002; Kim *et al.*, 2006; Watanabe *et al.*, 2010; Li *et al.*, 2011; Lin *et al.*, 2011) to estimate the relative importance of mobile ( $\text{NO}_x$  from motor vehicles) versus stationary ( $\text{SO}_2$  from fossil-fueled power plants) pollution emission sources (Li *et al.*, 2011). In our data, the  $\text{NO}_3^-/\text{SO}_4^{2-}$  - ratios are 0.65, 0.71 and 0.66 for CLM, LABS and KM, respectively, indicating that the fog composition is typically sulfate-dominated at these locations and that stationary power plants play a major role in acidifying the fog samples. Only at XT, the ratio is 1.04, which shows that mobile emission sources play a larger role at this site.

The main source of sodium and chloride is generally droplet-scavenging of sea salt (Li *et al.*, 2011), while another important source of non-sea-salt- $\text{Cl}^-$  in the air are emissions from coal burning and petrochemical factories (Lu *et al.*, 2010). Both ions were much more abundant at XT and KM than at CLM and LABS, respectively. The measured  $\text{Cl}^-/\text{Na}^+$  equivalent ratios were quite different from the respective ratio in sea water (1.17, Li *et al.*, 2011). The larger ratios at CLM, LABS and KM (median ratio 1.79, see Table 1) are caused by anthropogenic  $\text{Cl}^-$  emissions. The smaller ratio at XT indicates that  $\text{Cl}^-$  was driven from the aerosol phase into the gas phase (as HCl) after acidification of the fog water by anthropogenic sulfuric and nitric acids. Low  $\text{Cl}^-/\text{Na}^+$  equivalent ratios at XT were correlated to low pH's indicating that the respective acids lead to de-gassing of HCl.

Magnesium and calcium are both contained in sea salt, but their concentrations in the air are often dominated from long range dust transports and re-suspended road dust (Yang *et al.*, 2011) as well as from local construction sites, manufacturing, steel works and power plants (Li *et al.*, 2011). There is a clear maritime influence of sea salt on the  $\text{Mg}^{2+}$  concentration at XT and KM, while an additional nss-contribution is further evident at XT. The calcium appears to originate mostly from the maritime source at all sites.

**Table 1.** Fog event statistics and chemical compositions of fog water at all four sites in Taiwan.

		CLM	LABS	XT	KM
Number of fog samples		36	14	69	15
Number of fog events		18	13	17	2
Number of blanks		7	12	25	7
pH	Min	3.67	3.41	3.22	2.27
	Median	4.52	3.91	4.10	2.95
	Max	5.23	4.47	5.95	3.41
pAi	Min	3.09	2.96	1.71	1.97
	Median	3.99	3.48	2.89	2.92
	Max	5.08	3.97	3.74	3.02
Conductivity ( $\mu\text{S cm}^{-1}$ )	Min	4.70	40.5	48.3	317
	Median	31.6	103	358	453
	Max	165	312	2850	2810
LWC ( $\text{mg m}^{-3}$ )	Min	98.8	24.0	3.16	21.9
	Median	308	63.2	84.9	104
	Max	760	127	462	224
$\text{H}^+$ ( $\mu\text{eq L}^{-1}$ )	Min	5.89	33.9	1.12	389
	Median	30.6	125	79.4	1120
	Max	214	389	603	5370
$\text{Na}^+$ ( $\mu\text{eq L}^{-1}$ )	Min	bdl*	bdl*	11.0	25.4
	Median	bdl*	11.34	162	61.6
	Max	169	63.5	8140	3560
$\text{NH}_4^+$ ( $\mu\text{eq L}^{-1}$ )	Min	7.06	23.6	334	227
	Median	99.9	251	1300	469
	Max	614	655	14300	4610
$\text{K}^+$ ( $\mu\text{eq L}^{-1}$ )	Min	bdl*	2.76	6.81	10.7
	Median	2.80	17.9	35.7	15.1
	Max	25.2	33.1	581	193
$\text{Mg}^{2+}$ ( $\mu\text{eq L}^{-1}$ )	Min	0.823	2.88	1.79	3.81
	Median	3.70	9.71	47.5	14.3
	Max	51.4	18.9	2230	758
$\text{Ca}^{2+}$ ( $\mu\text{eq L}^{-1}$ )	Min	4.49	10.5	4.33	0.303
	Median	13.7	36.7	118	19.5
	Max	145	71.9	4500	422
$\text{Cl}^-$ ( $\mu\text{eq L}^{-1}$ )	Min	0.652	5.95	36.1	45.6
	Median	5.28	19.3	144	188
	Max	97.8	69.2	6130	3700
$\text{NO}_3^-$ ( $\mu\text{eq L}^{-1}$ )	Min	0.00	54.8	100	175
	Median	35.5	149	703	427
	Max	376	442	11500	5410
$\text{PO}_4^{3-}$ ( $\mu\text{eq L}^{-1}$ )	Min	bdl*	0.00	0.00	0.468
	Median	0.00	3.53	8.65	2.26
	Max	29.6	16.4	171	38.0
$\text{SO}_4^{2-}$ ( $\mu\text{eq L}^{-1}$ )	Min	4.22	53.4	89.4	638
	Median	57.8	212	682	842
	Max	591	919	8800	5290
TIC ( $\mu\text{eq L}^{-1}$ )	Min	36.2	272	683	2490
	Median	260	775	3210	3120
	Max	1720	2320	47100	29600
nss- $\text{SO}_4^{2-}$ ( $\mu\text{eq L}^{-1}$ )**	Min	4.22	53.4	82.3	630
	Median	57.3	212	673	838
	Max	587	919	8170	4860
nss- $\text{K}^+$ ( $\mu\text{eq L}^{-1}$ )**	Min	0.00	2.76	5.51	10.0
	Median	2.80	17.3	34.1	13.6
	Max	24.1	31.7	466	115
nss- $\text{Mg}^{2+}$ ( $\mu\text{eq L}^{-1}$ )**	Min	0.82	2.88	0.00	0.00
	Median	3.66	6.42	14.9	0.00

**Table 1.** (continued).

		CLM	LABS	XT	KM
nss-Ca <sup>2+</sup> (μeq L <sup>-1</sup> ) **	Max	19.2	14.9	650	66.3
	Min	4.49	10.5	3.06	0.00
	Median	13.7	35.8	112	14.1
	Max	143	71.5	4260	295
nss-Cl <sup>-</sup> (μeq L <sup>-1</sup> ) **	Min	(-99.4) ***	(-20.8) ***	(-3870) ***	(-534) ***
	Median	2.38	5.83	(-23.43) ***	36.7
	Max	12.7	18.6	87.40	347
Al (μg L <sup>-1</sup> )	Min	12.3	16.0	83.9	18.1
	Median	51.5	116	537	68.6
	Max	414	365	8390	794
Fe (μg L <sup>-1</sup> )	Min	30.0	40.0	17.5	44.1
	Median	75.0	160	867	96.7
	Max	150	440	8420	794
Ti (μg L <sup>-1</sup> )	Min	0.0827	0.763	1.39	0.183
	Median	1.18	3.04	8.38	3.18
	Max	8.73	10.8	101	63.1
V (μg L <sup>-1</sup> )	Min	0.540	2.72	1.11	7.72
	Median	2.02	4.40	9.43	30.7
	Max	8.11	11.7	54.7	108
Se (μg L <sup>-1</sup> )	Min	0.0921	0.300	2.32	2.25
	Median	0.465	1.42	5.17	5.06
	Max	3.03	3.50	36.4	25.1

\* “bdl” means “below detection limit”: Na<sup>+</sup>, K<sup>+</sup> and PO<sub>4</sub><sup>3-</sup> detection limits are 0.2 mg L<sup>-1</sup>.

\*\* nss-SO<sub>4</sub><sup>2-</sup> = SO<sub>4</sub><sup>2-</sup> - 0.12 Na<sup>+</sup>, nss-K<sup>+</sup> = K<sup>+</sup> - 0.022 Na<sup>+</sup>, nss-Mg<sup>2+</sup> = Mg<sup>2+</sup> - 0.227 Na<sup>+</sup>, nss-Ca<sup>2+</sup> = Ca<sup>2+</sup> - 0.044 Na<sup>+</sup>, nss-Cl<sup>-</sup> = Cl<sup>-</sup> - 1.17 Na<sup>+</sup> denote mean equivalent concentration ratios of the species of ions in seawater (Wang *et al.*, 2003; Watanabe *et al.*, 2006; Polkowska *et al.*, 2008; Jao, 2011, Li *et al.*, 2011).

\*\*\* nss-Cl<sup>-</sup> < 0 due to transformation of Cl<sup>-</sup> from the aerosol phase into the gas phase (as HCl) after acidification of the fog water by anthropogenic sulfuric and nitric acids. See text for more details.

Potassium is primarily emitted from biomass burning (Li *et al.*, 2011) and highest at XT. Phosphate, originating from soil dust and fertilizer use, was a minor constituent. Aluminum may originate from the earth’s crustal as well as from industrial sources. The main sources of iron in particles are steel industries and heavy fuel oil combustion (Hu *et al.*, 2015), while minor Fe, which is also a compound of minerals, may be of crustal origin (e.g., windblown soil dusts). Among the analyzed metals, Al and Fe were the dominant elements at all sites, while median concentrations were highest at XT (Al: 537 μg L<sup>-1</sup>, Fe: 867 μg L<sup>-1</sup>) and lowest at CLM (Al: 51.5 μg L<sup>-1</sup>, Fe: 75.0 μg L<sup>-1</sup>). Titanium is a crustal element as well, with frequent occurrence in mineral and fly ash (Hu *et al.* 2015). The Ti concentrations were low at all four sites, while highest at XT (8.38 μg L<sup>-1</sup>). Vanadium in the atmosphere originates mainly from the combustion of fossil fuels and ore processing (Teng *et al.* 2006). Visschedijk *et al.* (2013) reported for North-West Europe, that emissions are strongly concentrated at the densely populated cities with major sea ports, while the major sources for V are sea-going ships, petroleum refineries and industry. Median V concentrations of 30.7 μg L<sup>-1</sup> at KM were at least three times higher than at the other sites. The main sources of Selenium are fossil fuel combustion, waste incineration, copper refineries as well as chemical and glass industries (Ranville *et al.*, 2010; Hsu *et al.*, 2010). The Se concentrations showed a strongly positive correlation to the

SO<sub>4</sub><sup>2-</sup> concentrations supporting the hypothesis of common sources. Further, the median selenium concentrations were more than three times higher at XT and KM than at CLM and LABS, confirming their common source with sulfate, which was higher at XT and KM as well.

#### **pH and pAi Values and Fraction Acidity**

The median pH values in our fog samples range from 2.95 at KM site to 4.52 at CLM site. The median values of pAi range from 1.71 (XT) to 3.09 (CLM) and are often well below the pH values (Fig. 2(a)). At the two sites XT and KM, the pAi is almost the same (median 2.89 and 2.92, respectively), while the pH values at these two sites are very different from each other (4.10 versus 2.95). The major acidifying acid is sulfuric acid at CLM, LABS and KM (see SO<sub>4</sub><sup>2-</sup> concentrations in Table 1), while nitric acid is the dominating acidifier at XT (see NO<sub>3</sub><sup>-</sup> concentrations in Table 1). For KM, the difference between pAi and pH is very small (median difference 0.03), while high FA values (up to nearly 1.0 in some cases) indicate that the neutralizing effect of cations other than H<sup>+</sup> is negligible at this site and sulfuric acid and nitric acids are merely neutralized (Fig. 2(b)).

In contrast, the difference between pAi and pH is large (1.21 units) at XT, suggesting that the fog water would be much more acidic if there would not be a strong neutralization effect. This is supported by the low ratio FA as indicator of un-neutralized H<sup>+</sup>. High concentrations of ammonium



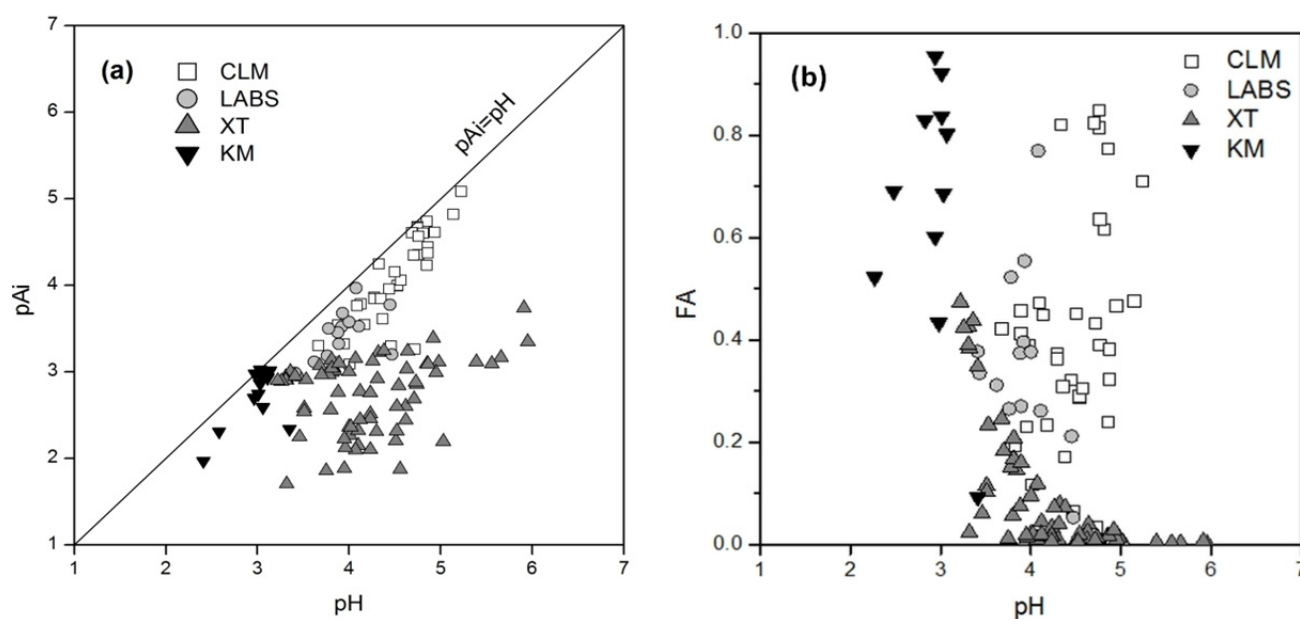


**Fig. 2.** Relations between pH and pAi (a), pH and FA (b) for all four sites

(median  $1300 \mu\text{eq L}^{-1}$ ) and the NF demonstrate that  $\text{H}^+$  at XT is nearly completely neutralized by  $\text{NH}_3$  through the formation of  $\text{NH}_4^+$ , while neutralization by  $\text{Ca}^{2+}$  and  $\text{Mg}^{2+}$  through  $\text{CaCO}_3$  and  $\text{MgCO}_3$  from the soil is weak.

For CLM and LABS, the differences between median pAi and median pH are 0.43 and 0.53, respectively. The fractional acidity of individual samples at CLM and LABS cover a relatively wide range between 0.03 and 0.85 at pH values between 3.41 and 5.23. Therefore, the sites CLM and LABS are between the extremes KM and XT.

The order of neutralization of acidic components is  $\text{NH}_4^+ > \text{Ca}^{2+} > \text{Mg}^{2+}$  at all sites.

### Sources of Pollutants and Air Mass Origins

The chemical composition of fog at a site varies with its air mass origins. By using the backward trajectories, typical air mass origins were defined for each site. To exclude dilution effects due to differences in LWC, the ion loadings (IL) were used for the discussion of chemical information in conjunction with air mass histories (see Table 2).

At CLM, the air masses were advected from various directions (Fig. 3(a)) and the trajectories were grouped into two regimes. While regime 1 covers air masses originating from Mainland China (24 samples), air masses classified as regime 2 exclusively traveled over the Pacific Ocean and the Taiwan Strait during the last 48 hours before reaching the study site (12 samples). The ion loadings of regime 1 were consistently higher than those of regime 2 for all ions (Table 2). Median ILs for dominant ions,  $\text{H}^+$ ,  $\text{NH}_4^+$ ,  $\text{NO}_3^-$  and  $\text{SO}_4^{2-}$  were 35%, 38%, 96% and 63% higher at regime 1 than at regime 2.

At LABS, the air masses mainly originated from either strictly westerly or strictly easterly direction. Consequently, they were divided into a regime 1, representing air masses travelling over Mainland China (9 samples), and a regime 2, with air masses of maritime origin (5 samples). Again, the

median ILs were higher for the air masses that had travelled over Mainland China, in this case by 9% for  $\text{H}^+$ , by 62% for  $\text{NH}_4^+$ , by 10% for  $\text{NO}_3^-$ , and by 68% for  $\text{SO}_4^{2-}$ .

For XT, a classification into a regime from West, one from North and one from East is an obvious choice. While the number of trajectories arriving from North is high and several of them are crossing Mainland China's coast line with its industrial hub at the Yangtze River Delta, four well distinguished regimes were used for data analysis instead of three. Regime 1 covers the air masses advected from Mainland China from west (1 fog event, 18 samples), regime 2 represents the air masses coming from North and crossing Chinese landmass (21 samples), regime 3 (22 samples) and regime 4 (8 samples) cover trajectories traveling over the ocean from North and East, respectively. The ILs of  $\text{H}^+$ ,  $\text{NH}_4^+$ , and  $\text{SO}_4^{2-}$  were highest at the regimes 1 and 2. The  $\text{NO}_3^-$  concentrations are ranked according to the order regime 1 > regime 3 > regime 2 > regime 4. Generally, total ILs decreased from regime 1 ( $507 \text{ neq m}^{-3}$ ) to regime 4 ( $180 \text{ neq m}^{-3}$ ), while the median LWC in regime 1, which is just representing one single fog event starting on October 7<sup>th</sup>, was more than five times higher than the ones of the other regimes ( $262 \text{ mg m}^{-3}$ ,  $44.3 \text{ mg m}^{-3}$ ,  $41.3 \text{ mg m}^{-3}$ ,  $48.5 \text{ mg m}^{-3}$ ).

At KM, all air masses arrived from the south and were advected from the Pacific Ocean south of Taiwan during the last 48 h before sampling. ILs in fog water of the fog event starting March 29<sup>th</sup> were much higher than in the fog event of April 13<sup>th</sup> (enhancement of 676% for  $\text{H}^+$ , 448% for  $\text{NH}_4^+$ , 287% for  $\text{NO}_3^-$  and 288% for  $\text{SO}_4^{2-}$ ). Generally ILs of the four dominating ions  $\text{H}^+$ ,  $\text{NH}_4^+$ ,  $\text{NO}_3^-$  and  $\text{SO}_4^{2-}$  as well as  $\text{nss-Ca}^{2+}$  and  $\text{nss-Mg}^{2+}$  were enhanced in the air masses advected from China Mainland at all sites.

### Comparison of Chemical Characteristics between the Sites

There is a large difference of fog water concentrations



**Table 2.** Median Ion Loadings in  $\text{neq m}^{-3}$  of major ions for each regime.

Ion	regimes CLM		regimes LABS		regimes XT				events KM	
	I: China	II: Sea	I: China	II: Sea	I: West (China)	II: North (China)	III: North	IV: East	I: March 27 <sup>th</sup>	II: April 13 <sup>th</sup>
Na <sup>+</sup>	0.00	0.00	0.577	1.18	4.65	38.5	31.5	8.13	8.28	30.8
NH <sub>4</sub> <sup>+</sup>	23.1	16.7	22.5	13.9	249	149	117	74.4	90.9	20.3
K <sup>+</sup>	0.880	0.00	1.17	0.718	4.63	3.65	3.72	1.88	2.42	1.64
Mg <sup>2+</sup>	0.992	0.757	0.683	0.607	1.00	14.9	8.08	1.51	1.89	6.85
Ca <sup>2+</sup>	3.98	2.27	1.95	1.20	2.02	25.7	11.0	5.45	0.77	4.49
Cl <sup>-</sup>	1.49	1.04	1.48	1.19	17.4	33.3	28.1	5.91	30.8	29.7
NO <sub>3</sub> <sup>-</sup>	9.44	4.81	10.0	9.12	89.7	75.9	82.8	33.7	86.4	30.1
PO <sub>4</sub> <sup>3-</sup>	0.00	0.00	0.134	0.230	0.00	1.06	0.813	0.172	0.293	0.547
SO <sub>4</sub> <sup>2-</sup>	20.5	12.6	21.3	12.7	122	95.7	63.2	46.6	131	45.4
H <sup>+</sup>	10.0	7.39	9.91	9.08	15.9	4.33	2.42	2.53	177	26.2
sum	70.4	45.6	69.7	49.9	507	442	349	180	530	196

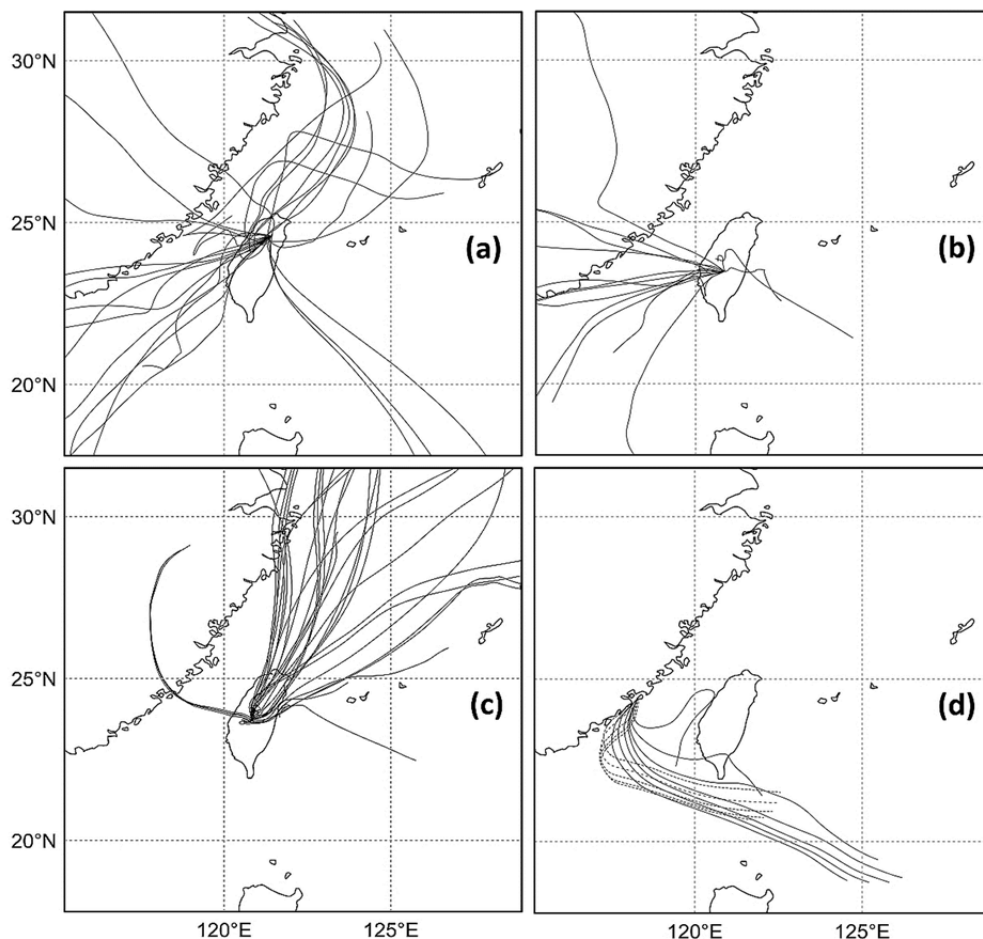


**Fig. 3.** Backward trajectories representing the last 48 hours before reaching the site at CLM (April 13<sup>th</sup> 2011 to May 24<sup>th</sup> 2011) (a), LABS (April 13<sup>th</sup> 2011 and May 17<sup>th</sup> 2011) (b), XT (September 9<sup>th</sup> 2013 and November 1<sup>st</sup> 2013) (c) and KM (event on March 27<sup>th</sup> 2014 with solid lines, event on April 13<sup>th</sup> 2014 with dotted lines) (d)

between the sites. The median concentrations of the dominating ions H<sup>+</sup>, NH<sub>4</sub><sup>+</sup>, NO<sub>3</sub><sup>-</sup> and SO<sub>4</sub><sup>2-</sup> are shown in Fig. 4(a) for direct comparability. The LWC varied largely between the sites as well. As mentioned before, the

differences in LWC between samples and between sites lead to a variable dilution of the ions in solution. The CLM site exhibited the highest LWC and the LABS site the lowest.

The CLM site is rather specific through low ILs and

high LWC. Its proximity to the sea causes a consistently high humidity, while its high altitude of 1650 m asl leads to strong cooling of air masses during adiabatic ascent and thus high LWC. During southwesterly winds, which dominate Taiwan during the southwest summer monsoon season from May to September, the site lies on the leeward side of the Central Taiwanese Mountain Range and is thus sheltered from winds from Mainland China. East of CLM is Ilan County, which is located in the mouth of the Lanyang River Valley. It is just weakly industrialized and has moderate agriculture (Chang *et al.*, 2002). For these reasons, the ion concentrations at CLM were comparatively low and are likely to be consistently low during the whole year. This presumption is supported by data by Beiderwieden *et al.* (2007), who collected fog water at CLM from August to September 2006, while the site was affected by northeasterly winds. The equivalent concentrations observed in 2006 are in the same order of magnitude as equivalent concentrations observed in 2011: median pH 4.13 versus pH 4.52 (2011,

this study), median EC 52.0 versus 31.6  $\mu\text{S cm}^{-1}$ , TIC 324 versus 260  $\mu\text{eq L}^{-1}$ ,  $\text{NH}_4^+$  56.3 versus 99.9  $\mu\text{eq L}^{-1}$ ,  $\text{NO}_3^-$  35.5 versus 35.5  $\mu\text{eq L}^{-1}$ , and  $\text{SO}_4^{2-}$  103 versus 57.8  $\mu\text{eq L}^{-1}$ , respectively. These ions dominate the ion balance, making up 85% (86%) of the total equivalent concentration at CLM.

The Lulin Atmospheric Background Station (LABS) shows the smallest LWC of all sites. The dominant fog type is a stratus cloud, which touches the mountain top during horizontal advection. Backward trajectory analysis shows that air masses can reach the rather exposed LABS site from several directions. The concentrations of all ions were higher at LABS than at CLM, with the median pH being lower. After converting the concentrations to ILs, the picture changes and the concentrations of ions per volume of air are very similar at CLM and LABS (Fig. 4(b)).

The XT site is the only site where samples were mostly taken under the influence of northeasterly winds during the winter monsoon in September and October. Therefore, most of the air masses were advected from North-East, whereas

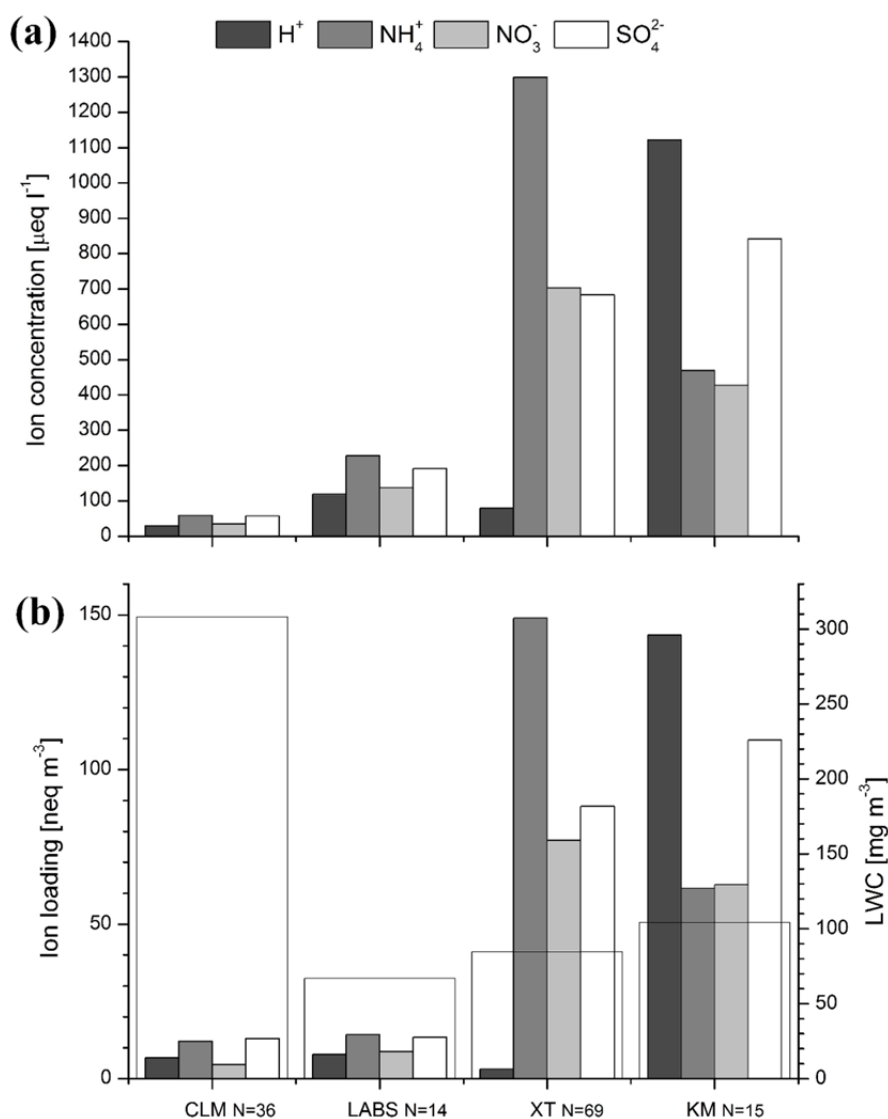


**Fig. 4.** Median ion concentrations of dominating ions  $\text{H}^+$ ,  $\text{NH}_4^+$ ,  $\text{NO}_3^-$  and  $\text{SO}_4^{2-}$  (a) and ion loadings of dominating ions  $\text{H}^+$ ,  $\text{NH}_4^+$ ,  $\text{NO}_3^-$  and  $\text{SO}_4^{2-}$  including median LWC (empty wide bars) (b).

only during one single fog event, the air was advected by westerly winds from Mainland China. This event showed high LWC and high ILs. In general, the pAi was low and the pH high at XT. The acidity was largely neutralized by the formation of ammonium from ammonia. This is related to sources from agriculture (Liang *et al.*, 2009) and traffic in the larger region. High concentrations of  $K^+$ , which are good indicators for biomass burning, underline the strong influence of agricultural-waste burning, in all likelihood burning of rice straw (Chen *et al.*, 2008). The median nitrate concentrations in XT were the highest compared to the other sites and were slightly higher than median  $SO_4^{2-}$  concentrations. Again, this shows the larger influence of  $NO_x$  emissions from nearby urbanized central-west Taiwan (Liang *et al.* 2009) and the greater Taipei region.

ILs of  $SO_4^{2-}$  at XT were not much lower than those observed at KM. Backward trajectory analysis suggests that ILs of  $SO_4^{2-}$  were highest in the air advected from Mainland China, from both westerly and northerly directions. High concentrations of  $Na^+$  and  $Cl^-$  as well as a high fraction of sea-salt- $Mg^{2+}$  indicate a maritime influence at XT.

Liang *et al.* (2009) analyzed fog samples in Xitou for an entire year and reported a median pH of 4.9, median TIC  $3390 \mu eq L^{-1}$ ,  $NH_4^+$   $630 \mu eq L^{-1}$ ,  $NO_3^-$   $510 \mu eq L^{-1}$  and  $SO_4^{2-}$   $760 \mu eq L^{-1}$ . The median and the maximum (not shown) ion concentrations in Liang *et al.* (2009) were mostly lower than the concentrations of our study (with the exception of median sulfate, which was about 10% higher). This discrepancy might be caused by different study designs.

The XT site was rather sheltered from northeastern winds by the central mountain range during our experimental period. It would definitively be worthwhile to analyze the differences in chemical composition and LWC of fog water between the southwesterly and northeasterly monsoon seasons. During the southwesterly monsoon season throughout the months of May to September, the fog water in XT might be even more polluted due to further advection of air masses from the West.

The air at KM has been described to be heavily polluted by industrial emissions from Mainland China (Hsu *et al.* 2010). During the field campaign from the end of March to mid-April, air masses during foggy conditions were exclusively advected from the Southeast and the South. Here, two fog events were sampled. Although their trajectories are not too much different from each other, the two events varied strongly in terms of median LWC and median ILs. The median LWC of the first event on March 29<sup>th</sup> was  $136 mg m^{-3}$ , while LWC of the second event on April 13<sup>th</sup> was  $25 mg m^{-3}$ . While the ion concentrations were higher in the second event, the ion loadings were higher in the first event. Similarly to the situation at CLM and LABS, the anion concentrations at KM were dominated by sulfate. A high fraction of nss- $Cl^-$  at KM (see Table 1), directly related to emissions from coal burning, clearly underlines the influence of anthropogenic sulfur emissions. Probably the relatively short travel distance along the Mainland China shore sufficed to introduce large amounts of air pollutants into our fog samples. Further investigation on chemical composition of fog water during winter conditions should be performed

since even higher air pollution is expected during winter, as suggested by Hsu *et al.* (2010).

Fog episodes are reported to contain extremely high metal loads and high diversity of metal-rich particle species. Most of the metals in fog typically originate from local emission sources (Hu *et al.*, 2015). This makes metals in fog water very good indicators for local anthropogenic pollution of fog water.

Aluminum in fog water commonly originates from soil material, ash and metal surfaces (Lewis, 1989), while Iron is reported to be among the dominating metal particles at other sites (Hu *et al.*, 2015). In Taiwan, the presence of Al and Fe is related to local emission sources, while advection of mineral soil dust from Mainland China, especially during northeasterly winter monsoon, occurs as well (Hsu *et al.*, 2010). At XT, this is consistent with high concentrations of  $Ca^{2+}$ . Other sources for the occurrence of Fe and Al at XT are likely the industry in Western Taiwan and the locally intensive agricultural activity with rather high exposure of soil and dust to the air.

The titanium concentrations are very low at all four sites, highest at XT which might be due to soil dust exposure through agricultural activity, regional industrial and traffic sources, or from long-range transport of dust from East Asia. Vanadium is much more present on Kinmen Island (KM) due to its position as a coastal site and its short distance to big harbors on Mainland China's coast. Selenium concentrations are several times higher at XT and KM than at CLM and LABS due to its relation to industrial fossil fuel combustion (Hsu *et al.* 2010).

## CONCLUSIONS

Fog samples were collected at the Chilan Mountain (CLM), Lulin Mountain (LABS), Xitou Experimental Forest (XT) and Kinmen Island (KM) sites in Taiwan to study the chemical composition of fog water. These investigations provide the first data on the chemical composition of fog water for LABS and KM sites and present the first comparison of four sites sampled with the same instrumental setups and sampling designs in Taiwan.

While the sites vary largely in terms of altitude above sea level, type of fog, and the potential sources of constituents in fog water, the chemical composition of fog water was clearly dominated by  $H^+$ ,  $NH_4^+$ ,  $NO_3^-$  and  $SO_4^{2-}$ , making up more than 85% of the TIC at all sites. The ion concentrations (ICs) at LABS were higher than those at CLM, however, the stations' results are very similar when ion loadings (ILs) are considered. The ICs and ILs at CLM and LABS were smaller than at XT and KM, as both CLM and LABS are situated in rural areas and just weakly influenced by local pollution sources. Considering the status of LABS as a background station, which is generally free from boundary layer pollution, the measured contamination of fog water, mainly by  $NH_4^+$ ,  $NO_3^-$  and  $SO_4^{2-}$  from anthropogenic sources, suggests the long-range transport of air pollutants from continental East Asia being an island-wide issue for Taiwan.

At XT, the relatively high median pH is caused by acid neutralization through ammonium, which originates from

NH<sub>3</sub> emissions from agriculture and other sources such as vehicular traffic. Furthermore, XT was the only site with a NO<sub>3</sub><sup>-</sup>/SO<sub>4</sub><sup>2-</sup>-ratio larger than unity, indicating a particularly large influence of NO<sub>x</sub> emissions from nearby urbanized central-west Taiwan and the greater Taipei region. Generally, the chemical composition of fog water at XT as a peripheral forest site, which is used for nature education as well as recreation, is obviously heavily affected by long-range transport of pollutants as well as rather local anthropogenic emissions.

At KM, the air is heavily polluted, and so is fog water as well. While moderate NO<sub>3</sub><sup>-</sup> and NH<sub>4</sub><sup>+</sup> ILs characterize KM as a rural site with little local population as well as few mobile and stationary nitrogen emissions, high ILs of SO<sub>4</sub><sup>2-</sup> suggest the influence of polluted air transported from Mainland China. High concentrations of SO<sub>4</sub><sup>2-</sup> at XT and KM are consistent with Mainland China's and Taiwan's continued active use of coal combustion for electric power generation (Li et al., 2011).

The analysis of the metal ions supports the picture of CLM and LABS as rural sites with less maritime influence and less pollution on one hand, and XT and KM with partly detectable maritime influence and strong anthropogenic pollution on the other. Whenever the air masses originated from Mainland China, the ion loadings and ion concentrations in fog water were high.

Changes in fog liquid phase ion concentrations (IC) as a function of variability in LWC were observed and are believed to be adequately considered by the use of atmospheric ion loadings (IL). Therefore, fog chemistry should be evaluated not only with ion concentrations, but also with ion loadings. Our study presents a good overview of the ion and metal concentrations in fog throughout Taiwan and the respective dominating factors and processes. Further studies should cover more chemical compounds, for example anhydrosugars in order to analyze the influence of biomass burning on fog chemistry, and organic pollutants to better resolve industrial sectors' influence on pollution in fog. Further, the two main monsoon seasons should be covered more representatively. This study may help to analyze future trends of fog chemistry as a result of pollutant emission control or changing LWC at given sites due to regional effects of global climate change.

## ACKNOWLEDGMENTS

The authors gratefully acknowledge the NOAA Air Resources Laboratory (ARL) for the provision of the HYSPLIT transport and dispersion model and/or READY website (<http://www.ready.noaa.gov>) used in this publication. Travel funds from the German Academic Exchange Service (DAAD) and support from our partners in Taiwan are gratefully acknowledged as well.

## REFERENCES

- Ali, K., Momin, G.A., Tiwari, S., Safai, P.D., Chate, D.M. and Rao, P.S.P. (2004). Fog and Precipitation Chemistry at Delhi, North India. *Atmos. Environ.* 38: 4215–4222.
- Beiderwieden, E., Klemm, O. and Hsia Y. (2007). The Impact of fog on the Energy Budget of a Subtropical Cypress Forest in Taiwan. *Taiwan J. For. Sci.* 22: 227–239.
- Chang, S.C., Lai, I.L. and Wu, J.T. (2002). Estimation of Fog Deposition on Epiphytic Bryophytes in a Subtropical Montane Forest Ecosystem in Northeastern Taiwan. *Atmos. Res.* 64: 159–167.
- Chang, S.C., Yeh, C.F., Wu, M.J., Hsia, Y.J. and Wu, J.T. (2006). Quantifying Fog Water Deposition by in Situ Exposure Experiments in a Mountainous Coniferous Forest in Taiwan. *For. Ecol. Manage.* 224: 11–18.
- Chen, K.S., Wang, H.K., Peng, Y.P., Wang, W.C. and Lai, C.H. (2008). Effects of Open Burning of Rice Straw on Concentrations of Atmospheric Polycyclic Aromatic Hydrocarbons in Central Taiwan. *J. Air Waste Manage. Assoc.* 58: 1318–1327.
- Collett Jr., J.L., Hoag, K.J., Sherman, D.E., Bator, A. and Richards, L.W. (1999a). Spatial and Temporal Variations in San Joaquin Valley Fog Chemistry. *Atmos. Environ.* 33: 129–140.
- Collett Jr., J.L., Hoag, K.J., Rao, X. and Pandis, S.N. (1999b). Internal Acid Buffering in San Joaquin Valley Fog Drops and Its Influence on Aerosol Processing. *Atmos. Environ.* 33: 4833–4847.
- Collett, Jr., J.L., Bator, A., Sherman, D.E., Moore, K.F., Hoag, K.J., Demoz, B.B., Rao, X. and Reilly, J.E. (2002). The Chemical Composition of Fogs and Intercepted Clouds in the United States. *Atmos. Res.* 64: 29–40.
- Daum, P.H., Kelly, T.J., Schwartz, S.E. and Newman, L. (1984). Measurements of the Chemical Composition of Stratiform Clouds. *Atmos. Environ.* 18: 2671–2684.
- Degeffie, D.T., El-Madany, T.S., Held, M., Hejkal, J., Hammer, E., Dupont, J.C., Haeffelin, M., Fleischer, E. and Klemm, O. (2015). Fog Chemical Composition and its Feedback to Fog Water Fluxes, Water Vapor Fluxes and Microphysics in the Evolution of Two Events near Paris. *Atmos. Res.* 164–165: 328–338.
- Draxler, R.R. and Hess, G.D. (1998). An Overview of the Hysplit 4 Modeling System for Trajectories, and Deposition. *Aust. Meteorol. Mag.* 47: 295–308.
- Elbert, W., Hoffmann, M.R., Kraemer, M., Schmitt, G. and Andreae, M.O. (2000). Control of Solute Concentrations in Cloud and Fog Water by Liquid Water Content. *Atmos. Environ.* 34: 1109–1122.
- El-Madany, T.S., Griessbaum, F., Fratini, G., Juang, J.Y. and Chang, S.C. (2013). Comparison of Sonic Anemometer Performance under Foggy Conditions. *Agric. For. Meteorol.* 173: 63–73.
- Giulianelli, L., Gilardoni, S., Tarozzi, L., Rinaldi, M., Decesari, S., Carbone, C., Facchini, M.C. and Fuzzi, S. (2014). Fog Occurrence and Chemical Composition in the Po valley over the Last Twenty Year. *Atmos. Environ.* 98: 394–401.
- Gonser, S., Klemm, O., Griessbaum, F., Chang, S.C., Chu, H.S. and Hsia, Y.J. (2011). The Relation between Humidity and Liquid Water Content in Fog: An Experimental Approach. *Pure Appl. Geophys.* 169: 821–833.
- Hara, H. (1993). Acid Deposition Chemistry in Japan. *Bull. Inst. Public Health* 42: 426–437.

- Hara, H., Kitamura, M., Mori, A., Noguchi, I., Ohizumi, T., Seto, S., Takeuchi, T. and Deguchi, T. (1995). Precipitation Chemistry in Japan 1989–1993. *Water Air Soil Pollut.* 85: 2307–2312.
- Herckes, P., Wortham, H., Mirabel, P. and Millet, M. (2002). Evolution of the Fogwater Composition in Strasbourg (France) from 1990 to 1999. *Atmos. Res.* 64: 53–62.
- Herckes, P., Marcotte, A., Wang, Y. and Collett J.L. (2015). Fog Composition in the Central Valley of California over Three Decades. *Atmos. Res.* 151: 20–30.
- Hsu, S.C., Liu, S.C., Tsai, F., Engling G., Lin, I.I., Chou, C.K.C., Kao, S.J., Lung, S.C.C., Chan, C.Y., Lin S.C., Huang, J.C., Chi, K.H., Chen, W.N., Lin, F.J., Huang, C.H., Kuo, C.L., Wu, T.C. and Huang, Y.T. (2010). High Wintertime PM Pollution over an Offshore Island (Kinmen) off Southeastern China: An Overview. *J. Geophys. Res.* 115.
- Hu, Y., Lin, J., Zhang, S., Kong, L., Fu, H. and Chen, J. (2015). Identification of the Typical Metal Particles among Haze, Fog, and Clear Episodes in the Beijing Atmosphere. *Sci. Total Environ.* 511: 369–380.
- Jacob, D.J., Munger, J.W., Waldman, J.M. and Hoffmann, M.R. (1986).  $\text{H}_2\text{SO}_4$  –  $\text{HNO}_3$  –  $\text{NH}_3$  System at High Humidities and in Fogs, Part 1, Spatial and Temporal Patterns in the San Joaquin Valley of California. *J. Geophys. Res.* 91: 1073–1088.
- Johnson, C.A., Sigg, L. and Zobrist, J. (1987). Case studies on the Chemical Composition of Fogwater: The Influence of Local Gaseous Emissions. *Atmos. Environ.* 21: 2365–2374.
- Joos, F. and Baltensperger, U. (1991). A Field Study on Chemistry, S(IV) Oxidation Rates and Vertical Transport during Fog Conditions. *Atmos. Environ.* 25: 217–230.
- Kim, M.G., Lee, B.K. and Kim, H.J. (2006). Cloud/Fog Water Chemistry at a High Elevation site in South Korea. *J. Atmos. Chem.* 55: 13–29.
- Klemm, O., Wrzesinsky, T., Gerchau, J. and Griebbaum, F. (2008). A Collector for Fog Water and Interstitial Aerosol. *J. Atmos. Oceanic Technol.* 25: 335–340.
- Lai, I.L., Chang, S.C., Lin, P.H., Chaou, C.H. and Wu, J.T. (2006). Climatic Characteristics of the Subtropical Mountainous Cloud Forest at the Yuanyang Lake Long-Term Ecological Research Site, Taiwan. *Taiwania* 51: 317–329.
- Lee, C.T., Chuang, M.T., Lin, N.H., Wang, J.L., Sheu, G.R., Chang, S.C., Wang, S.H., Huang, H., Chen, H.W., Liu, Y.L., Weng, G.H., Lai, H.Y. and Hsu, S.P. (2011). The Enhancement of  $\text{PM}_{2.5}$  Mass and Water-soluble Ions of Biosmoke Transported from Southeast Asia over the Mountain Lulin Site in Taiwan. *Atmos. Environ.* 45: 5784–5794.
- Lewis, T.E. (1989). *Environmental Chemistry and Toxicology of Aluminum*. CRC Press.
- Li, P., Li, X., Yang, C., Wang, X., Chen, J. and Collett Jr., J.L. (2011). Fog Water Chemistry in Shanghai. *Atmos. Environ.* 45: 4034–4041.
- Liang, Y.L., Lin, T.C., Hwong, J.L., Lin, N.H. and Wang, C.P. (2009). Fog and Precipitation Chemistry at a Mid-land Forest in Central Taiwan. *J. Environ. Qual.* 38: 627–636.
- Lin, N.H. and Peng, C.M. (1998). Chemistry of Mountain Clouds Observed in the Northern Taiwan. In Proceedings of the 1<sup>st</sup> International Conference of Fog and Fog Collection, Vancouver, 19–24 July 1998, pp. 117–120.
- Lin, N.H., Jao, J.C. and Peng, C.M. (2010). A 15-year Dataset of Mountain Cloud Chemistry Observation in Northern Taiwan. In Proceedings of the 5th International Conference of Fog, Fog Collection and Dew, Münster, Germany, 25–30 July 2010, p. 298.
- Lu, C., Niu, S., Tang, L., Lv, J., Zhao, L. and Zhu, B. (2010). Chemical Composition of Fog Water in Nanjing area of China and its Related Fog Microphysics. *Atmos. Res.* 97: 47–69.
- Polkowska, Ż., Błaś, M., Klimaszewska, K., Sobik, M., Małek, S. and Namieśnik, J. (2008). Chemical Characterization of Dew Water Collected in Different Geographic Regions of Poland. *Sensors* 8: 4006–4032.
- Ranville, M.A., Cutter, G.A., Buck, C.S., Landing, W.M., Cutter, L.S., Resing, J.A. and Flegal, A.R. (2010). Aeolian Contamination of Se and Ag in the North Pacific from Asian Fossil Fuel Combustion. *Environ. Sci. Technol.* 44: 1587–1593.
- Seinfeld, J.H. and Pandis, S.N. (2006). *Atmospheric Chemistry and Physics. From Air Pollution to Climate Change. Second Edition*. John Wiley & Sons, New Jersey.
- Sheu, G.R., Lin, N.H., Wang, J.L., Lee, C.T., Ou Yang C.F. and Wang, S.H. (2010). Temporal Distribution and Potential Sources of Atmospheric Mercury Measured at a High-elevation Background Station in Taiwan. *Atmos. Environ.* 44:2393–2400.
- Tago, H., Kimura, H., Kozawa, K. and Fuije, K. (2006). Longterm Observation of Fogwater Composition at Two Mountainous Sites in Gunma Prefecture, Japan. *Water Air Soil Pollut.* 175: 375–391.
- Teng, Y., Ni, S., Zhang, C., Wang, J., Lin, X. and Huang, Y. (2006). Environmental Geochemistry and Ecological Risk of Vanadium Pollution in Panzhihua Mining and Smelting Area, Sichuan, China. *Chin. J. Chem.* 25: 4.
- Visschedijk, A.H.J., Denier van der Gon, H.A.C., Hulskotte, J.H.J. and Quass, U. (2013). Anthropogenic Vanadium Emissions To air and Ambient Air Concentrations in North-West Europe. In Proceedings of the 16<sup>th</sup> International Conference on Heavy Metals in the Environment Rome, Italy, September 23–27, E3S Web of Conferences 1, 030004.
- Wai, K.M., Lin, N.H., Wang, S.H. and Dokiya, Y. (2008). Rainwater Chemistry at a High-altitude Station, Mt. Lulin, Taiwan: Comparison with a Background Station, Mt. Fuji. *J. Geophys. Res.* 113.
- Wang, G., Wang, H., Yu, Y., Gao, S., Feng, J., Gao, S. and Wang, L. (2003). Chemical Characterization of Water-Soluble Components of  $\text{PM}_{10}$  and  $\text{PM}_{2.5}$  Atmospheric Aerosols in Five Locations of Nanjing, China. *Atmos. Environ.* 37: 2893–2903.
- Wang, Y., Zhang, J., Marcotte, A.R., Karl, M., Dye, C. and Herckes, P. (2015). Fog Chemistry at Three Sites in Norway. *Atmos. Res.* 151: 72–81.
- Watanabe, K., Takebe, Y., Sode, N., Igarashi, Y., Takahashi,

- H. and Dokiya, Y. (2006). Fog and Rain Water Chemistry at Mt. Fuji: A Case Study during the September 2002 Campaign. *Atmos. Res.* 82: 652–662.
- Watanabe, K., Honoki, H., Iwai, A., Tomatsu, A., Noritake, K., Miyashita, N., Yamada, K., Yamada, H., Kawamura, H. and Aoki, K. (2010). Chemical Characteristics of Fog Water at Mt. Tateyama, near the Coast of the Japan Sea in Central Japan. *Water Air Soil Pollut.* 211: 379–393.
- World Meteorological Organization (2004). Manual for the Gaw Precipitation Chemistry Programme. <ftp://ftp.wmo.int/Documents/PublicWeb/arep/gaw/gaw160.pdf>, Last Access: 16 June 2015.
- Wrzesinsky, T. and Klemm, O. (2000). Summertime Fog Chemistry at a Mountainous Site in Central Europe. *Atmos. Environ.* 34: 1487–1496.
- Yang, J.Y., Xie, C.E., Shi, C.E., Liu, D.Y., Niu, S.J. and Li, Z.H. (2011). Ion Composition of Fog Water and its Relation to Air Pollutants during Winter Fog Events in Nanjing, China. *Pure Appl. Geophys.* 169: 1037–1052.
- Zhang, Z., Gao, J., Engling, G., Tao, J., Chai, F., Zhang, L., Zhang, R., Sang, X., Chan, C., Lin, Z. and Cao, J. (2015). Characteristics and Application of Size-segregated Biomass Burning Tracers in China's Pearl River Delta Region. *Atmos. Environ.* 102: 290–301.

*Received for review, March 10, 2015*

*Revised, July 10, 2015*

*Accepted, August 12, 2015*